How to cite: *Angew. Chem. Int. Ed.* **2020**, *59*, 21909–21914
International Edition: doi.org/10.1002/anie.202008943
German Edition: doi.org/10.1002/ange.202008943

Membranes

Ultrafast Semi-Solid Processing of Highly Durable ZIF-8 Membranes for Propylene/Propane Separation

Qiang Ma[+], Kai Mo[+], Shushu Gao, Yafang Xie, Jinzhao Wang, Hua Jin, Armin Feldhoff, Shutao Xu, Jerry Y. S. Lin, and Yanshuo Li**

Abstract: *ZIF-8 membranes have emerged as the most promising candidate for propylene/propane (C_3H_6/C_3H_8) separation through its precise molecular sieving characteristics. The poor reproducibility and durability, and high cost, thus far hinder the scalable synthesis and industrial application of ZIF-8 membranes. Herein, we report a semi-solid process featuring ultrafast and high-yield synthesis, and outstanding scalability for reproducible fabrication of ZIF-8 membranes. The membranes show excellent C_3H_6/C_3H_8 separation performance in a wide temperature and pressure range, and remarkable stability over 6 months. The ZIF-8 membrane features dimethylacetamide entrapped ZIF-8 crystals retaining the same diffusion characteristics but offering enhanced adsorptive selectivity for C_3H_6/C_3H_8. The ZIF-8 membrane was prepared on a commercial flat-sheet ceramic substrate. A prototypical plate-and-frame membrane module with an effective membrane area of about 300 cm^2 was used for efficient C_3H_6/C_3H_8 separation.*

Propylene–propane separation is one of the most significant but challenging processes in chemical industry.[1] Membrane-based separations hold tremendous superiority as compared with the energy-intensive cryogenic distillation process.[2] Typical polymer membranes are subjected to the trade-off between permeability and selectivity which is known as Robeson's upper bound.[3] In contrast, microporous inorganic membranes with outstanding molecular sieving properties have the potential to exceed the Robeson's upper limit.[4] Metal-organic framework (MOF) membranes, for one, have been demonstrated to be capable of kinetic separation of H_2/CO_2,[5] CO_2/N_2,[6] CO_2/CH_4[7] and olefin/paraffin[8] mixtures, owing to the well-defined pore structures and precisely tunable functionality for adsorbate affinity.

Zeolitic imidazolate framework-8 (ZIF-8), consisting of zinc ions coordinated with 2-methylimidazolate ligands,[9] is the most extensively studied MOF for membrane application. Owing to its structural flexibility, the effective pore aperture (4.0–4.2 Å) of ZIF-8 is larger than the crystallographically determined aperture (3.4 Å), exhibiting the great potential in kinetic separation for propylene/propane (4.03/4.16 Å).[10] The ideal kinetic selectivity for propylene/propane on ZIF-8 is measured to be 125 by Li et al. in 2009.[11] In 2012, the first ZIF-8 membrane for highly efficient propylene/propane separation was reported by Lai et al., with propylene permeability up to 200 Barrer and separation factor up to 50.[12] Several groups around the world have greatly advanced the development of ZIF-8 membranes after that.[13–19] For example, Jeong and co-workers have developed series of methods for the synthesis of ZIF-8 membranes, including counter-diffusion method,[13] microwave assisted seeded growth,[14] rapid thermal deposition (RTD) method.[15] Nair and co-workers developed an interfacial microfluidic membrane processing (IMMP) for parallelizable fabrication of MOF membranes inside polymeric hollow-fiber substrates.[16] Recently, Tsapatsis and co-workers reported ligand-induced permselectivation (LIPS) process for synthesis of ZIF-8 membranes on γ-alumina supports.[17] Most of the reported performance have already met the industrial application requirements, i.e., C_3H_6 permeability higher than 1 Barrer and C_3H_6/C_3H_8 selectivity higher than 35.[20] Nevertheless, there are still several challenges remaining to be overcome towards industrial applications, including reduction of membrane cost, improvement of process reproducibility, long-term membrane durability, and more importantly, modularization with high packing density.[21]

Herein, we report a reliable and scalable semi-solid processing approach, i.e., dip coating-thermal conversion (DCTC) method (Figure 1a) for the fabrication of ZIF-8 membranes. The precursor solution was prepared by dissolving stoichiometric metal and ligand in H_2O/DMAc (dimethylacetamide) mixed solvent. It should be noted that the preparation should be carried out in an ice-bath in the first 300 min so as to achieve an inhibition of nucleation (Figure S2). This is the key step to guarantee a uniform coating of ZIF-8 separating layer and high reproducibility of membrane

[*] Q. Ma,[+] K. Mo,[+] Y. Xie, J. Wang, Dr. H. Jin, Prof. Dr. Y. Li
School of Materials Science and Chemical Engineering, Ningbo University
Ningbo 315211 (China)
E-mail: jinhua@nbu.edu.cn
liyanshuo@nbu.edu.cn
S. Gao, Prof. Dr. S. Xu
National Engineering Laboratory for Methanol to Olefins, Dalian National Laboratory for Clean Energy, Dalian Institute of Chemical Physics, Chinese Academy of Sciences
Dalian 116023 (China)
Prof. Dr. A. Feldhoff
Institute of Physical Chemistry and Electrochemistry, Leibniz University Hannover
Callinstraße 3A, 30167 Hannover (Germany)
Prof. Dr. J. Y. S. Lin
School for Engineering of Matter, Transport and Energy, Arizona State University
Tempe, AZ 85287 (USA)
[+] These authors contributed equally to this work.
Supporting information and the ORCID identification number(s) for the author(s) of this article can be found under: https://doi.org/10.1002/anie.202008943.

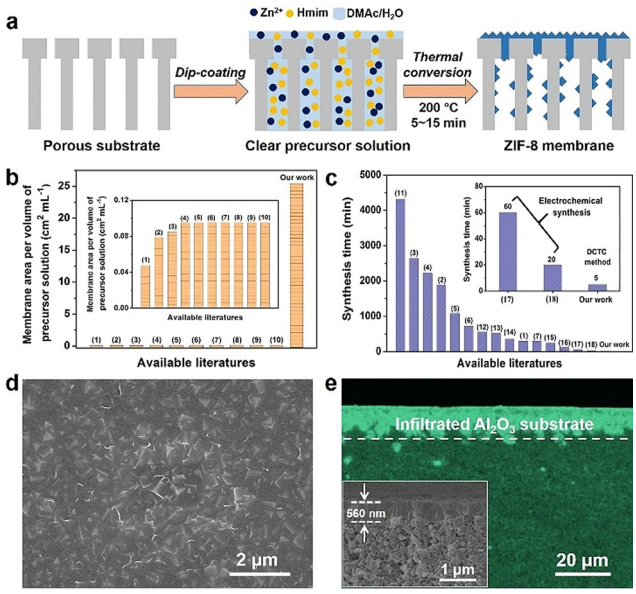

Figure 1. a) Schematic diagram of the dip coating-thermal conversion (DCTC) method for fabricating ZIF-8 membranes. Literature values and those of this work for: b) the production of membrane area pre volume of precursor solution and c) synthesis time for the fabrication of ZIF-8 membranes (Table S1 in the Supporting Information). d) Top view SEM image and e) the cross-sectional EDXS-mapping of the ZIF-8 membrane (Zn is marked in green. Inset: the cross-sectional SEM image).

preparation. A porous alumina ceramic support was dip-coated into the clear precursor solution. After a short thermal conversion treatment at 200 °C, ZIF-8 membrane was obtained. The method features the total utilization of the precursors. Thus, the productivity of DCTC method (defined as the production of total membrane area divided by the volume of the precursor solution) far exceeds that of solution-based synthesis, which was extremely advantageous in terms of cost and waste reduction (Figure 1 b). The DCTC method enables thus far the most rapid preparation with a very short duration of 5 min (Figure 1 c). In addition, DCTC synthesis is carried out in an open atmosphere. Tsapatsis and co-workers indicated that compared with solvothermal or hydrothermal synthesis, solvent-free and seed-free methods hold the advantages in term of scalability. They developed a ligand-induced permselectivation method for preparing ZIF-8 membranes based on atom layer deposition (ALD) processing.[17] But the ALD processing still faces with great challenges upon scalable synthesis. In short, the ultrafast semi-solid synthesis, demonstrated here, offers great potential to be applied in the continuous, large-scale preparation of ZIF-8 membranes.

The as-synthesized ZIF-8 membrane has a pure ZIF-8 phase according to X-ray diffraction (Figure S3). The membrane surface is completely covered by homogenous ZIF-8 crystals (Figure 1 d), revealing a crack-free microstructure. The 560 nm thick ZIF-8 membrane exhibits a thin film interference phenomenon analogous to the literature,[22] which could be an indication of moderate thickness fitly falling in the wavelength ranges of visible light (Figure S4). In the dip-coating procedure, the porous support was almost filled with precursor solution. Concentration-gradient-driven flow of the precursor solution from inside of support to outside nourishes the ZIF-8 layer to form defect-free ZIF-8 membrane. Meanwhile, plenty of ZIF-8 existed in the porous substrate as well (Figure 1 e), contributing to the enhanced adhesion as well as mechanical strength of the ZIF-8 membrane.

The ZIF-8 membrane features a sharp cut-off between C_3H_6 and C_3H_8 as intended (Figure 2 a), and the ideal selectivities for H_2/CH_4, H_2/C_3H_8 and C_3H_6/C_3H_8 (36.2, 8192 and 221, respectively) far exceeds their corresponding Knudsen selectivities (2.83, 4.69 and 1.02, respectively). Besides, the C_3H_6 permeance of 5.2×10^{-9} mol m^{-2} s^{-1} Pa^{-1} and C_3H_6/C_3H_8 separation factor of 190 was achieved on the ZIF-8 membrane for binary C_3H_6/C_3H_8 mixture separation (25 °C, 1 bar), confirming the excellent quality of the ZIF-8 membrane. To meet the requirement for practical application, vacuum operation for C_3H_6/C_3H_8 binary mixture separation was performed as well, showing the basically same separation performance as sweeping gas operation (Table S2). The C_3H_6/C_3H_8 separation performance of the ZIF-8 membranes is beyond most of polymer and zeolite as well as carbon-based membranes, and also comparable to the previous ZIF-8 reported membranes (Figure 2 b and Table S3).

Integrating membrane separation with distillation could result in 10–50 % reduction in the operating costs for C_3H_6/C_3H_8 separation.[23] To this end, the membranes must withstand high pressure ($\approx$20 bar) and elevated temperature (>50 °C) without significant performance reduction. Up-to-now, most of the reported separation performance of ZIF-8 membrane were measured at atmosphere and room temperature. Significant decrease of C_3H_6/C_3H_8 selectivity at high pressure was reported by different authors.[24] Opposite to the previous reports, the membrane synthesized by DCTC method shows a gradually increased C_3H_6/C_3H_8 separation factor from 190 to 250, when feed pressure increases from 1 to 7 bar (Figure 2 c). The distinctive phenomenon could be elucidated in terms of enhanced adsorption of C_3H_6 which hinders the C_3H_8 transport through ZIF-8 membrane. On the other side, the as-synthesized ZIF-8 membrane possibly possesses rigid framework.[7b,25] Both the C_3H_6 and C_3H_8 permeance decreases with increasing feed pressure, which could be ascribed to non-linear adsorption isotherms of C_3H_6 and C_3H_8 on ZIF-8.[10a] When temperature increased, the C_3H_6 permeance decreases slightly as opposed to the increased C_3H_8 permeance, resulting in the accordingly decreased C_3H_6/C_3H_8 separation factor (Figure 2 d). At elevated temperature, the reduced adsorption ability of ZIF-8 membrane for C_3H_6 accounts for the decreased C_3H_6 permeance. In contrast, the C_3H_8 permeance is improved due to the reduced blocking effect of preferentially transported C_3H_6 molecule. Nevertheless, the ZIF-8 membrane still possesses a moderate C_3H_6/C_3H_8 separation factor of about 25 at 150 °C, which could basically satisfy the separation factor requirement for industrial application.

Significantly, the separation performance can totally turn back when pressure or temperature go back to normal, suggesting the outstanding stability of ZIF-8 membrane. Moreover, the ZIF-8 membrane demonstrates excellent

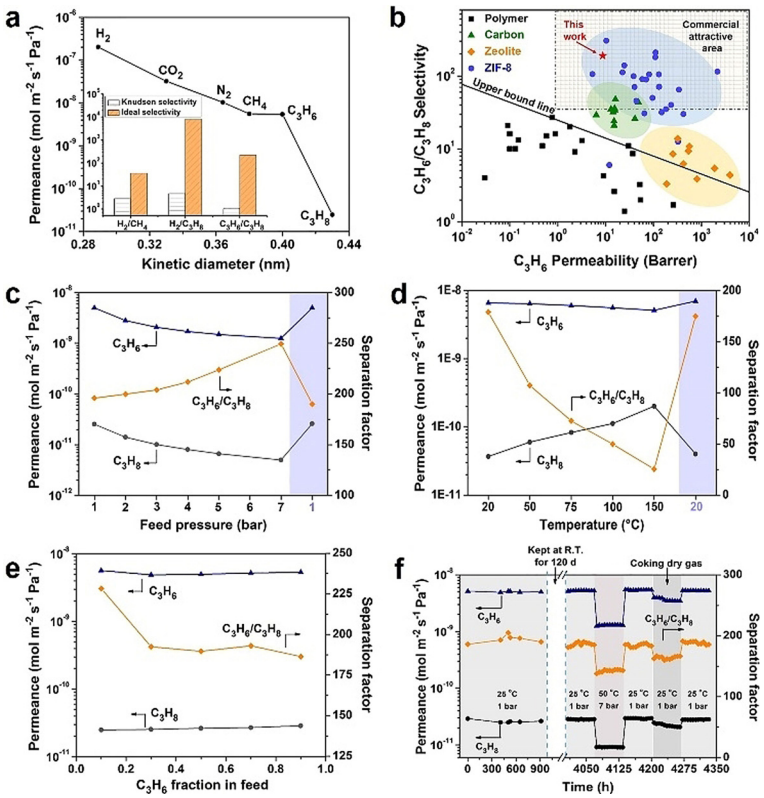

Figure 2. a) Single-gas permeance of the ZIF-8 membrane as a function of the gas kinetic diameter. b) The C_3H_6/C_3H_8 separation performance of the ZIF-8 membrane and of other reported systems, 1 Barrer = 3.4×10^{-16} mol m^{-2} s^{-1} Pa^{-1}. The shaded area in the graph represents the commercial attractive area for membrane performance (a minimum permeability of 1 Barrer and selectivity of 35).[20] The black line is the upper bound limit for polymer membranes. The binary C_3H_6/C_3H_8 separation performance of the ZIF-8 membrane as function of c) feed pressure, d) temperature, and e) C_3H_6 fraction in feed. f) Long-term stability of the ZIF-8 membrane for C_3H_6/C_3H_8 separation.

separation performances over a wide range of C_3H_6 fraction as well (Figure 2e). The remarkable membrane durability is highly expected for industrial application. Lin et al. reported stable operation ($\approx$40 days) of ZIF-8 membrane for C_3H_6/C_3H_8 separation at 35 °C and normal pressure.[24b] Herein, the ZIF-8 membrane furtherly exhibits outstanding long-term stability over a span of about 6 months (Figure 2f). The separation performance of the ZIF-8 membrane only fluctuates within a narrow range in the nearly one-month continuous test. Even after a long off-stream storage time (120 days), the membrane still remains excellent C_3H_6/C_3H_8 separation performance at elevated temperature (50 °C) and pressure (7 bar). In addition, the ZIF-8 membrane remains propylene-selective toward the coking dry gas (C_3H_6 20.3%, C_3H_8 49.6%, i-C_4H_{10} 4.0%, n-C_4H_{10} 16.0% and C_4H_8 10.1%) with C_3H_6/C_3H_8 separation factor of 160.

In order to identify the difference between the ZIF-8 membrane synthesized by DCTC method and conventional ZIF-8 membranes, the adsorption and diffusion of propylene and propane on different ZIF-8 was investigated. The ZIF-8 prepared by DCTC method has plenty of guest molecules in its cavities, as indicated by the much lower BET surface area (182 m^2 g^{-1}) than conventional ZIF-8 (1291 m^2 g^{-1}) and also the missing larger cavity (Figure 3a). The different relative intensity for *110/211* X-ray reflections also confirms the presence of molecular occupants in the ZIF-8 cages (Figure S5). ^{13}C NMR spectra provide a direct evidence (chemical shift of 23.6 ppm) that residual DMAc, the solvent used during the synthesis, exists in the cavities of ZIF-8 (Figure S6). Notably, the evident higher chemical shifts changes from 20.8 and 169.7 to 23.6 and 178.3 ppm, respectively, are observed as compared with dissociative DMAc molecule, proving the strong interaction between DMAc and the ZIF-8 framework. The TG-MS analysis shows the DMAc decomposing and leaving around 300 °C (Figure S7), which is in agreement with the ^{13}C NMR result. In addition, the preservation of C=O absorption peak around 1650 cm^{-1} in the thermally treated samples also implies the excellent thermal stability of embedded DMAc in the cavity of ZIF-8 below 200 °C. (Figure S8).

The confined DMAc has profound effect on the adsorption ability of ZIF-8. The DMAc embedded ZIF-8 (DMAc@ZIF-8) adsorbed preferably propylene to propane with the equilibrium C_3H_6/C_3H_8 uptake ratio of 2.72 at 273 K, which is higher than 1.07 as observed for conventional ZIF-8 (Figure 3b). The identical results are also obtained at 293 K (Figure S9). The DMAc@ZIF-8 exhibits Ideal Adsorbed Solution Theory (IAST) selectivity of 8.73 for equimolar C_3H_6/C_3H_8 mixture, again much higher than 1.06 for conventional ZIF-8 (Figure 3c and Figure S10). The dynamic breakthrough curves for equimolar C_3H_6/C_3H_8 mixture on the two ZIF-8 samples are clearly quite different. The conventional ZIF-8 is ineffective in thermodynamic separation of C_3H_6/C_3H_8 mixture with the basically same breakthrough time (Figure 3d), which is identical with the previous report.[26] Nevertheless, the DMAc@ZIF-8 shows good selectivity for C_3H_6 over C_3H_8, as confirmed by the longer breakthrough time of C_3H_6 than C_3H_8 (Figure 3e). The dynamic adsorption capacities are 21.40 and 6.40 mg g^{-1} for C_3H_6 and C_3H_8, respectively, close to the static IAST adsorption capacity (Table S4). Furthermore, the much higher Q_{st} value for C_3H_6 compared to C_3H_8 implies that the embedded DMAc effectively enhances the interaction between C_3H_6 and the ZIF-8 framework (Figure S11). One concern for DMAc@ZIF-8 might be its long-term stability. It is noteworthy that the DMAc molecules are in situ impregnated within the cages of ZIF-8 during DCTC processing. The achieved DMAc@ZIF-8 demonstrates excellent stability, as indicated by (1) DMAc leaving above 300 °C from TG-MS analysis, and (2) stable performance for 6 months.

The diffusion property of ZIF-8 membrane was estimated from the permeance and adsorption isotherms of C_3H_6 and C_3H_8. Notably, considering the impact of infiltrated ZIF-8 within substrate on gas permeance, the actual permeance of C_3H_6 and C_3H_8 on the top ZIF-8 layer was obtained with a correction made by the resistance-in-series model

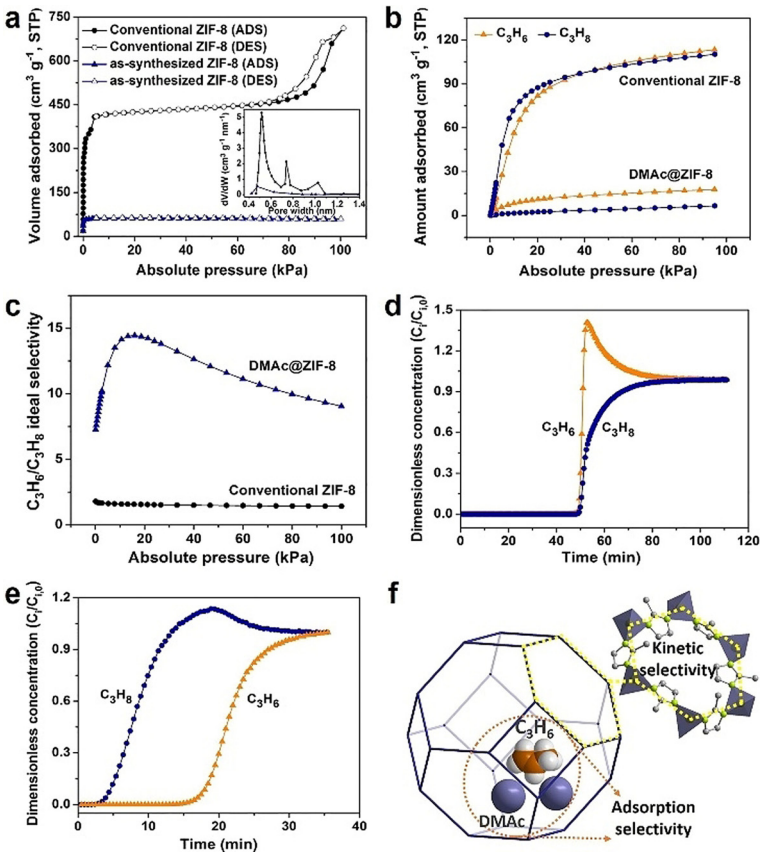

Figure 3. a) N_2 adsorption–desorption isotherms of ZIF-8 powders (the inset shows the corresponding pore size distribution). b) Adsorption isotherms and c) the IAST adsorption selectivities of ZIF-8 for C_3H_6/C_3H_8. Experimental breakthrough curves for the equimolar C_3H_6/C_3H_8 mixture (273 K, 1 bar) on the packed-bed column: d) conventional ZIF-8 and e) DMAc@ZIF-8. f) Schematic representation of the DMAc@ZIF-8 for C_3H_6/C_3H_8 separation.

(Table S5). Plots of C_3H_6 or C_3H_8 flux versus $q_1(1+b_1P_f)+q_2(1+b_2P_f)$ and $\ln(1+bP_f)$ using the Dual-site Langmuir (DSL) and Langmuir adsorption models parameters, respectively, are given in Figure S12. The calculated diffusivities for C_3H_6 and C_3H_8 are comparable to the reported data (Table S6), indicating that the confined DMAc molecules cause negligible effect on gas diffusion. The result is in accordance with many reported literatures that gas diffusion coefficients is independent with the loaded guest molecules in ZIF-8 cavity.[27] For ZIF-8, it is the six-membered-ring aperture, not the cage, that defines the kinetic separation of C_3H_6 and C_3H_8. Thus, embedding DMAc in the cages (about 4 molecules/cage according to TG data) should not affect C_3H_6 and C_3H_8 diffusion in ZIF-8. The permeation selectivity can be expressed as the product of the adsorption selectivity (S_{ads}) and diffusion selectivity (S_{diff}).[28] Thus, the synergistic effect of adsorption and diffusion herein contributes to the remarkable separation property of DMAc@ZIF-8 membrane for C_3H_6/C_3H_8 (Figure 3 f).

The ultrafast and semi-solid synthesis endows DCTC process with great superiority in scaling-up synthesis compared with conventional solvothermal method. The generality and scalability of DCTC process for ZIF-8 membrane were further explored on commercial substrates. Flat-sheet ceramic substrates were employed for scaling-up synthesis considering their better mechanical strength compared with polymeric supports and much higher packing density compared with tubular ceramic supports. The resultant flat-sheet ZIF-8 membrane (80×80 mm size) shows well-intergrown but unsmoothed microstructure (Figure S13), due to the rough substrate surface (Figure S14). Nevertheless, these membranes still show satisfactory C_3H_6/C_3H_8 separation factor around 40 (Table S7). Moreover, the DCTC method displays excellent reproducibility between different batches. A prototypical plate-and-frame module composed of three ZIF-8 flat-sheet membranes with effective membrane area larger than 300 cm^2 was successfully fabricated and tested for C_3H_6/C_3H_8 separation (Figure 4). Feed gas (C_3H_6 200 mL min^{-1} and C_3H_8 200 mL min^{-1}) and sweep gas N_2 (200 mL min^{-1}) were simultaneously fed to the membrane module. C_3H_6 permeance of 2.4×10^{-9} mol m^{-2} s^{-1} Pa^{-1} and C_3H_6/C_3H_8 separation factor of 38 measured on this module. The module performance is almost identical to the single flat-sheet ZIF-8 membrane, demonstrating the feasibility of ZIF-8 membrane for large scale applications.

For inorganic membranes capable of molecular separation, the commercial applications have been mainly limited to LTA zeolite membranes for organic solvent dehydration. Under industrial operation conditions, the zeolite membranes offer a typical water flux of about 1–5 kg m^{-2} h^{-1} (with H_2O/organic selectivity larger than 500). Extrapolated to 20 bar, the flux of the modularized ZIF-8 membranes is estimated to be 0.1 kg m^{-2} h^{-1}. Considering that the packing density of flat-sheet membrane (≈250 m^2 m^{-3}) is 5 times higher than that of the tubular zeolite membranes (≈50 m^2 m^{-3}), to commercialize our ZIF-8 membranes, the target is to further improve the membrane permeance by 2 to 10 times. Thus, reducing membrane thickness, especially the intermediate layer thickness, would be our next focus.

In summary, a semi-solid process featured with ultrafast and high-yield synthesis, and outstanding scalability has been developed for fabricating ZIF-8 membranes. The resultant ZIF-8 membranes exhibit precise molecular sieving for C_3H_6/C_3H_8 separation with separation factor of 190. The outstanding separation performance and reliable durability was demonstrated as well by the prolonged measurement over a span of 6 months. The synthesis of high-quality ZIF-8 membranes on commercial flat sheet ceramic substrate was successfully achieved with high reproducibility. A prototypical plate-and-frame ZIF-8 membrane module with membrane area larger than 300 cm^2 has been implemented for efficient separation of propylene and propane, foreshadowing the bright future of scalable ZIF-8 membrane for commercial applications.

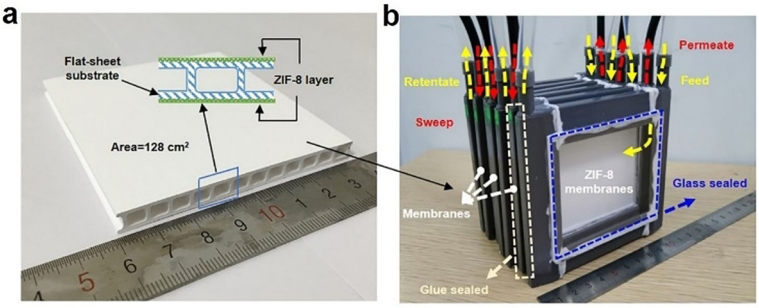

c

Membrane	C_3H_6 permeance ($\times 10^{-9}$ mol m^{-2} s^{-1} Pa^{-1})	C_3H_6/C_3H_8 selectivity
M1	2.7	45.3
M2	2.6	45.9
M3	2.4	35.1
Module	**2.4**	**38.0**

Figure 4. Digital photos of a) a flat-sheet ZIF-8 membrane and b) a prototypical plate-and-frame membrane module. c) C_3H_6/C_3H_8 separation performance of the plate-and-frame module and each individual flat-sheet membrane.

Acknowledgements

This work was supported by the National Natural Science Foundation of China (No. 21808113), National Natural Science Foundation of Zhejiang (No. LR18B060002), Major Special Projects of the Plan "Science and Technology Innovation 2025" in Ningbo (No. 2018B10016) and the K. C. Wong Magna Fund in Ningbo University. Gratefully acknowledged is funding by the Deutsche Forschungsgemeinschaft (DFG, German Research Foundation)—FE928/15-1.

Conflict of interest

The authors declare no conflict of interest.

Keywords: membranes · plate-and-frame module · propylene/propane separation · semi-solid processing · ZIF-8

[1] D. S. Sholl, R. P. Lively, *Nature* **2016**, *532*, 435 – 437.
[2] a) W. J. Koros, G. K. Fleming, *J. Membr. Sci.* **1993**, *83*, 1 – 80; b) R. W. Baker, B. T. Low, *Macromolecules* **2014**, *47*, 6999 – 7013.
[3] a) L. M. Robeson, *J. Membr. Sci.* **1991**, *62*, 165 – 185; b) L. M. Robeson, *J. Membr. Sci.* **2008**, *320*, 390 – 400; c) R. L. Burns, W. J. J. Koros, *J. Membr. Sci.* **2003**, *211*, 299 – 309.
[4] a) J. Shen, G. Liu, K. Huang, W. Jin, K.-R. Lee, N. Xu, *Angew. Chem. Int. Ed.* **2015**, *54*, 578 – 582; *Angew. Chem.* **2015**, *127*, 588 – 592; b) M. Lee, S. Hong, D. Kim, E. Kim, K. Lim, J. C. Jung, H. Richter, J. H. Moon, N. Choi, J. Nam, J. Choi, *ACS Appl. Mater. Interfaces* **2019**, *11*, 3946 – 3960; c) Y. Wang, H. Jin, Q. Ma, K. Mo, H. Mao, A. Feldhoff, X. Cao, Y. Li, F. Pan, Z. Jiang, *Angew. Chem. Int. Ed.* **2020**, *59*, 4365 – 4369; *Angew. Chem.* **2020**, *132*, 4395 – 4399.
[5] a) Y. Li, F. Liang, H. Bux, A. Feldhoff, W. Yang, J. Caro, *Angew. Chem. Int. Ed.* **2010**, *49*, 548 – 551; *Angew. Chem.* **2010**, *122*, 558 – 561; b) Y. Peng, Y. Lin, Y. Ban, H. Jin, W. Jiao, X. Li, W. Yang, *Science* **2014**, *346*, 1356 – 1359; c) Y. Sun, Y. Liu, J. Caro, X. Guo, C. Song, Y. Liu, *Angew. Chem. Int. Ed.* **2018**, *57*, 16088 – 16093; *Angew. Chem.* **2018**, *130*, 16320 – 16325.
[6] a) H. Yin, J. Wang, Z. Xie, J. Yang, J. Bai, J. Lu, Y. Zhang, D. Yin, J. Y. S. Lin, *Chem. Commun.* **2014**, *50*, 3699 – 3701; b) W. Wu, Z. Li, Y. Chen, W. Li, *Environ. Sci. Technol.* **2019**, *53*, 3764 – 3772.
[7] a) Q. Hou, Y. Wu, S. Zhou, Y. Wei, J. Caro, H. Wang, *Angew. Chem. Int. Ed.* **2019**, *58*, 327 – 331; *Angew. Chem.* **2019**, *131*, 333 – 337; b) D. J. Babu, G. He, J. Hao, M. T. Vahdat, P. A. Schouwink, M. Mensi, K. V. Agrawal, *Adv. Mater.* **2019**, *31*, 1900855.
[8] a) O. Shekhah, R. Swaidan, Y. Belmabkhout, M. D. Plessis, T. Jacobs, L. J. Barbour, I. Pinnau, M. Eddaoudi, *Chem. Commun.* **2014**, *50*, 2089 – 2092; b) A. Knebel, B. Geppert, K. Volgmann, D. I. Kolokolov, A. G. Stepanov, J. Twiefel, P. Heitjans, D. Volkmer, J. Caro, *Science* **2017**, *358*, 347 – 351.
[9] K. S. Park, Z. Ni, A. P. Cote, J. Y. Choi, R. D. Huang, F. J. Uribe-Romo, H. K. Chae, M. O'Keeffe, O. M. Yaghi, *Proc. Natl. Acad. Sci. USA* **2006**, *103*, 10186 – 10191.
[10] a) C. Zhang, R. P. Lively, K. Zhang, J. R. Johnson, O. Karvan, W. J. Koros, *J. Phys. Chem. Lett.* **2012**, *3*, 2130 – 2134; b) Y. C. Pan, Z. P. Lai, *Chem. Commun.* **2011**, *47*, 10275 – 10277.
[11] K. Li, D. H. Olson, J. Seidel, T. J. Emge, H. Gong, H. Zeng, J. Li, *J. Am. Chem. Soc.* **2009**, *131*, 10368 – 10369.
[12] Y. C. Pan, T. Li, G. Lestari, Z. P. Lai, *J. Membr. Sci.* **2012**, *390*, 93 – 98.
[13] a) H. T. Kwon, H. K. Jeong, *J. Am. Chem. Soc.* **2013**, *135*, 10763 – 10768; b) M. J. Lee, H. T. Kwon, H. K. Jeong, *Angew. Chem. Int. Ed.* **2018**, *57*, 156 – 161; *Angew. Chem.* **2018**, *130*, 162 – 167.
[14] a) H. T. Kwon, H. K. Jeong, *Chem. Commun.* **2013**, *49*, 3854 – 3856; b) H. T. Kwon, H. K. Jeong, A. S. Lee, H. S. An, T. Lee, E. Jang, J. S. Lee, J. Choi, *Chem. Commun.* **2016**, *52*, 11669 – 11672.
[15] M. N. Shah, M. A. Gonzalez, M. C. McCarthy, H. K. Jeong, *Langmuir* **2013**, *29*, 7896 – 7902.
[16] a) J. Brown, N. A. Brunelli, K. Eum, F. Rashidi, J. R. Johnson, W. J. Koros, C. W. Jones, S. Nair, *Science* **2014**, *345*, 72 – 75; b) K. Eum, A. Rownaghi, D. Choi, R. R. Bhave, C. W. Jones, S. Nair, *Adv. Funct. Mater.* **2016**, *26*, 5011 – 5018.
[17] X. Ma, P. Kumar, N. Mittal, A. Khlyustova, P. Daoutidis, K. A. Mkhoyan, M. Tsapatsis, *Science* **2018**, *361*, 1008 – 1011.
[18] a) W. Li, P. Su, Z. Li, Z. Xu, F. Wang, H. Ou, J. Zhang, G. Zhang, E. Zeng, *Nat. Commun.* **2017**, *8*, 406; b) W. Li, W. Wu, Z. Li, J. Shi, Y. Xia, *J. Mater. Chem. A* **2018**, *6*, 16333 – 16340.
[19] a) S. Zhou, Y. Wei, L. Li, Y. Duan, Q. Hou, L. Zhang, L. Ding, H. Wang, J. Xue, J. Caro, *Sci. Adv.* **2018**, *4*, eaau1393; b) R. Wei, H.-Y. Chi, X. Li, D. Lu, Y. Wan, C. Yang, Z. P. Lai, *Adv. Funct. Mater.* **2020**, *30*, 1907089.
[20] a) C. W. Colling, G. A. Huff, J. V. Bartels, US patent **2004** 20040000513; b) Z. P. Lai, *Curr. Opin. Chem. Eng.* **2018**, *20*, 78 – 85.
[21] Y. S. Lin, *Ind. Eng. Chem. Res.* **2019**, *58*, 5787 – 5796.
[22] E. Barankova, X. Tan, L. F. Villalobos, E. Litwiller, K. V. Peinemann, *Angew. Chem. Int. Ed.* **2017**, *56*, 2965 – 2968; *Angew. Chem.* **2017**, *129*, 3011 – 3014.
[23] R. Zarca, A. Ortiz, D. Gorri, L. T. Biegler, I. Ortiz, *J. Membr. Sci.* **2018**, *556*, 321 – 328.
[24] a) K. Eum, C. Ma, A. Rownaghi, C. W. Jones, S. Nair, *ACS Appl. Mater. Interfaces* **2016**, *8*, 25337 – 25342; b) D. Liu, X. Ma, H. Xi, Y. S. Lin, *J. Membr. Sci.* **2014**, *451*, 85 – 93; c) L. Sheng, C. Wang, F. Yang, L. Xiang, X. Huang, J. Yu, L. Zhang, Y. C. Pan, Y. S. Li, *Chem. Commun.* **2017**, *53*, 7760 – 7763.
[25] Q. Hou, S. Zhou, Y. Wei, J. Caro, H. Wang, *J. Am. Chem. Soc.* **2020**, *142*, 9582 – 9586.
[26] U. Böhme, B. Barth, C. Paula, A. Kuhnt, W. Schwieger, A. Mundstock, J. Caro, M. Hartmann, *Langmuir* **2013**, *29*, 8592 – 8600.

[27] a) T. Chokbunpiam, S. Fritzsche, C. Chmelik, J. Caro, W. Janke, *J. Phys. Chem. C* **2016**, *120*, 23458 – 23468; b) D. Freude, N. Dvoyashkina, S. S. Arzumanov, D. I. Kolokolov, A. G. Stepanov, C. Chmelik, H. Jin, Y. Li, J. Kärger, J. Haase, *J. Phys. Chem. C* **2019**, *123*, 1904 – 1912.
[28] a) R. Krishna, J. M. van Baten, *J. Membr. Sci.* **2010**, *360*, 323 – 333; b) S. Friebe, N. Wang, L. Diestel, Y. Liu, A. Schulz, A. Mundstock, J. Caro, *Microporous Mesoporous Mater.* **2015**, *216*, 127 – 132.

Manuscript received: June 27, 2020
Accepted manuscript online: August 25, 2020
Version of record online: September 28, 2020

